



Multilayer Metasurface Simulation in FDTD using Surface Susceptibility Model

Xiao Jia, Fan Yang*, Maokun Li, Shenheng Xu

Department of Electronic Engineering, Tsinghua University, Beijing, China



Copyright

©The use of this work is restricted solely for academic purposes. The author of this work owns the copyright and no reproduction in any form is permitted without written permission by the author.



Abstract

Multilayer designs of metasurfaces are required for practical applications because they have more capability to manipulate electromagnetic wave than single-layer designs. Here thus extend the Surface Susceptibility Model (SSM) integrated in FDTD from single layer to multilayers, consequently accelerating metasurfaces simulations with good accuracy. The SSM is integrated in FDTD by using Generalized Sheet Transition Conditions (GSTCs). To demonstrate the validity of the proposed algorithm, a numerical comparison is presented between simulation of two layer geometrical structures in conventional FDTD and two layer surface susceptibility model in FDTD-SSM.

Keyword: Metasurfaces, GSTCs, FDTD, surface susceptibilities



Biography



Xiao Jia received the B.S. degree from Northwestern Polytechnical University, Xi'an, China, the M.S. degree from University of Chinese Academy of Sciences, Beijing, China, in 2013 and 2016, respectively, She received the Ph.D. degree from Tsinghua University, Beijing, China, in 2020, under the supervision of Prof. Fan Yang. From 2018 to 2019, she was a visiting student at Polytechnique Montréal, Montréal, Québec, Canada, with the supervision of Prof. Christophe Caloz.

She is currently a lecturer at Beijing Jiaotong University, Beijing, China. Her current research interests include computational electromagnetics, metasurfaces, computational electromagnetics, reflectarray and transmitarray.

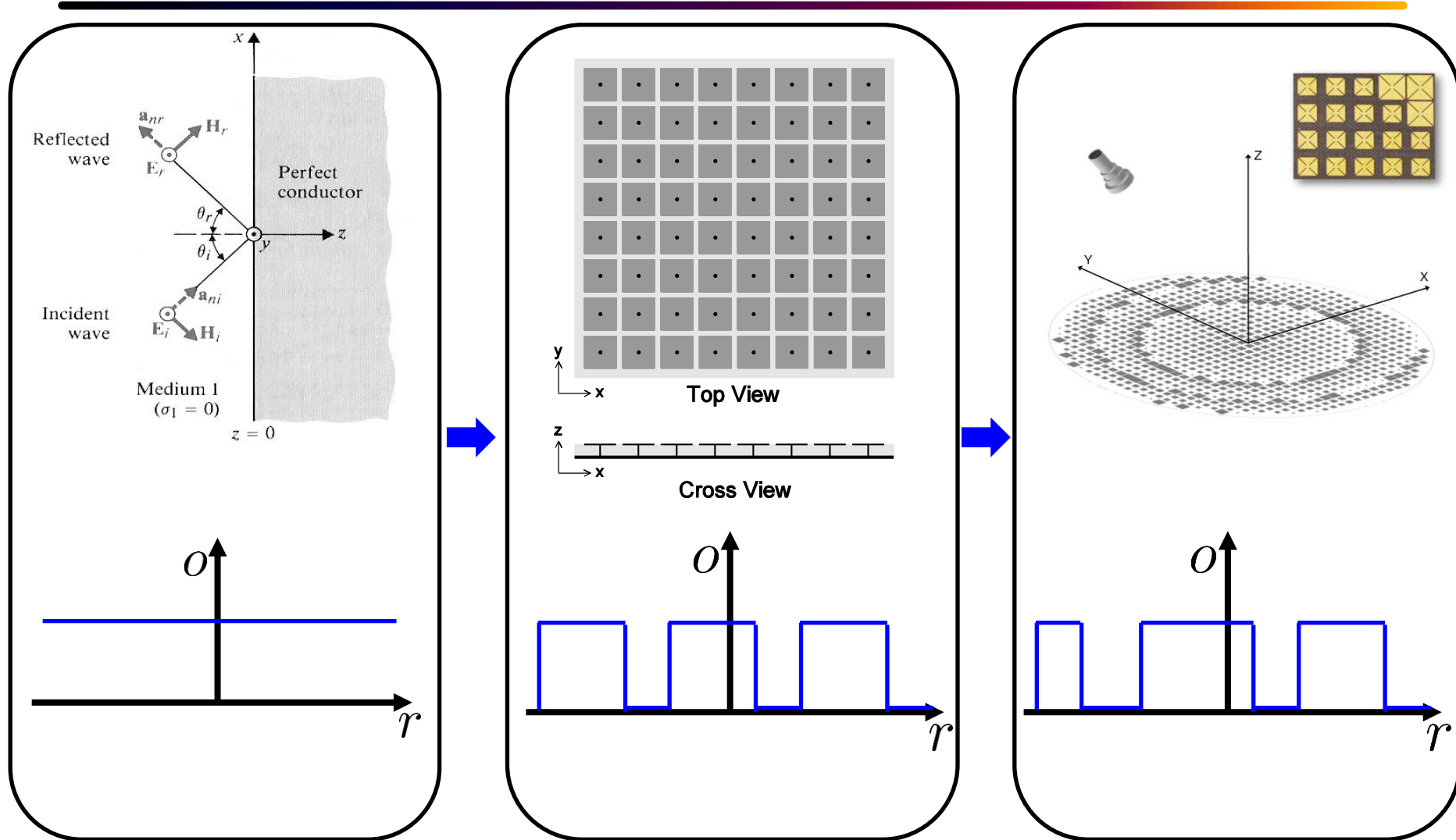


Outline

- ◆ Introduction of Metasurfaces
- ◆ Surface Susceptibility Model
- ◆ FDTD-SSM Algorithm
- ◆ Numerical Experiments
- ◆ Conclusion



Development of Metasurfaces



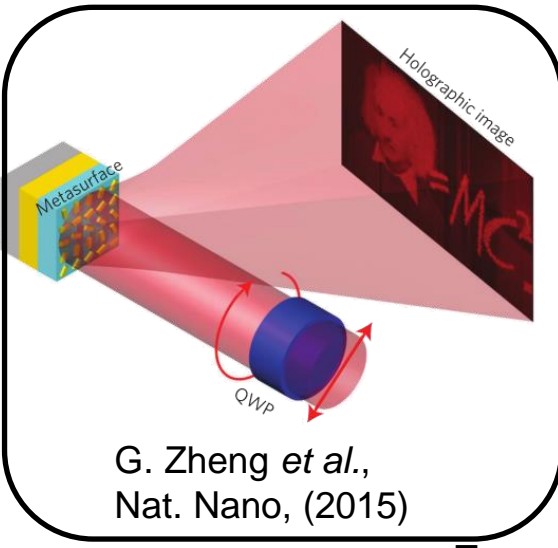
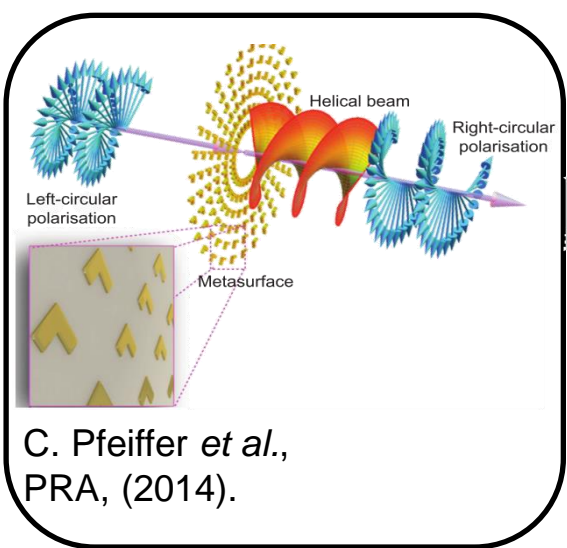
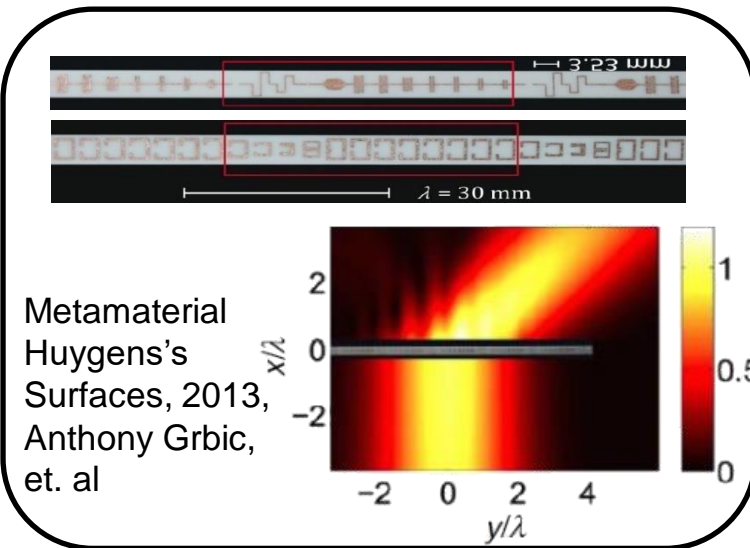
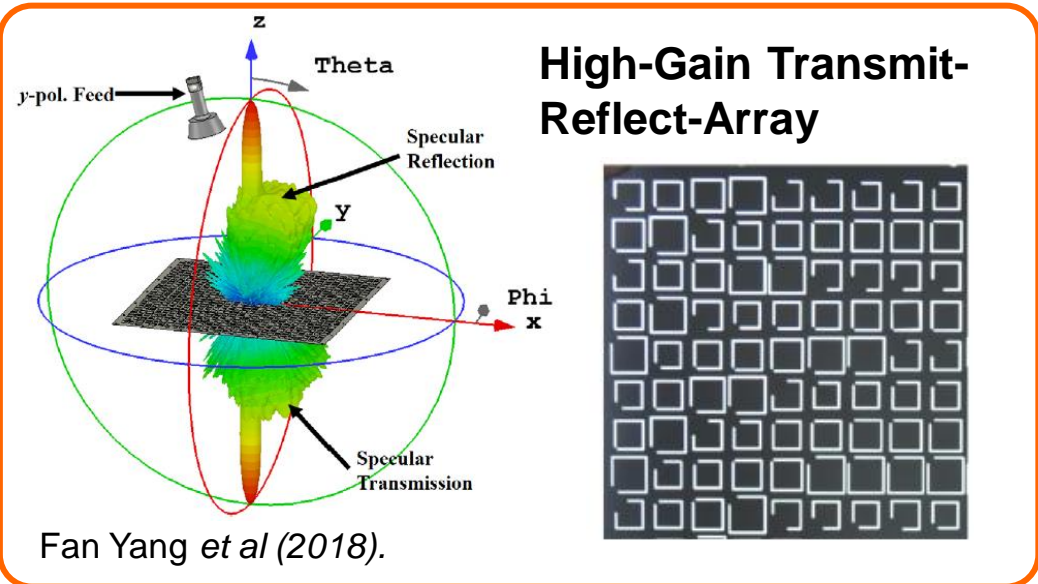
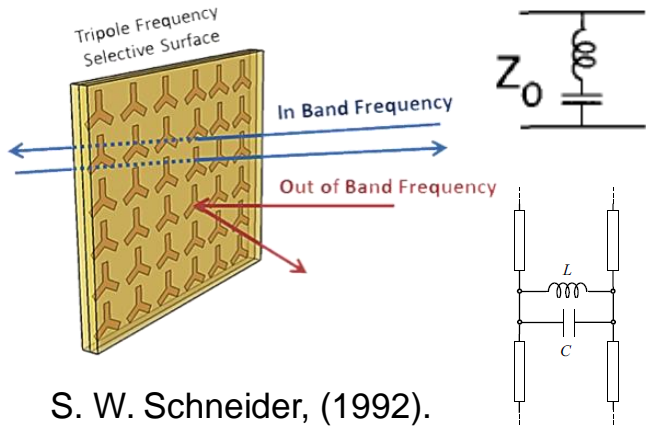
Ref: Yang F, Rahmat-Samii Y. Reflection phase characterizations of the EBG ground plane for low profile wire antenna applications[J]. IEEE Transactions on antennas and propagation, 2003, 51(10): 2691-2703.

Ref: Nayeri P, Yang F, Elsherbeni A Z. Reflectarray antennas: theory, designs, and applications[M]. John Wiley & Sons, 2018.



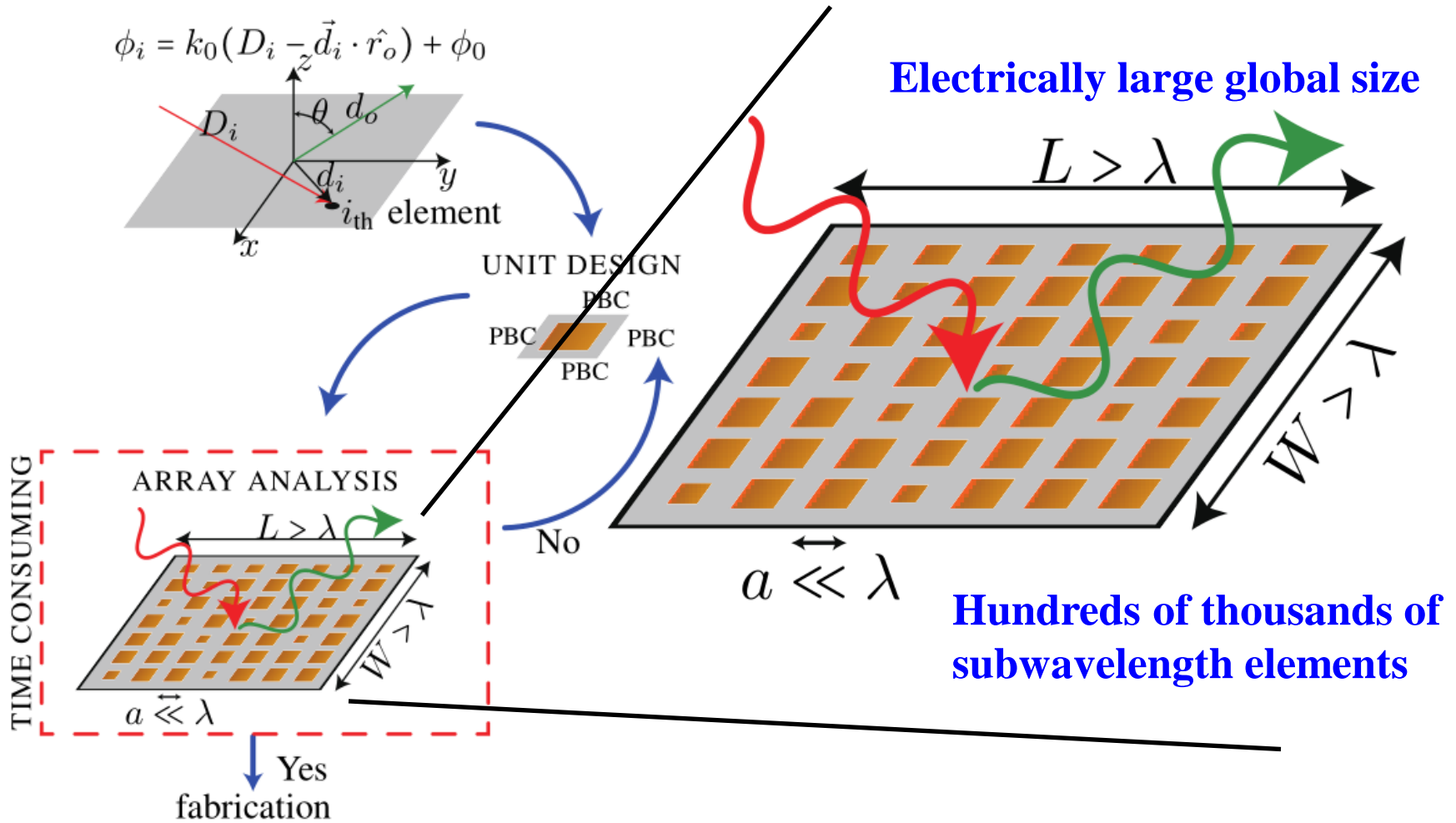
Applications

Frequency Selective Surfaces (FSSs)





Computational Challenges of Metasurfaces



Extremely dense meshes and huge number of unknowns leads to enormous computational problems.

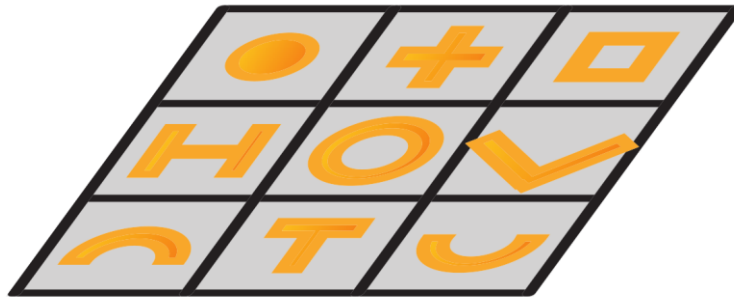


Outline

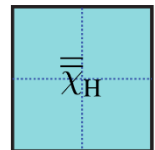
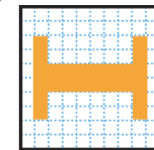
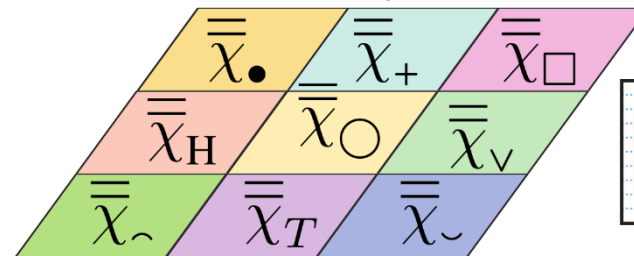
- ◆ Introduction of Metasurfaces
- ◆ Surface Susceptibility Model
- ◆ FDTD-SSM Algorithm
- ◆ Numerical Experiments
- ◆ Conclusion



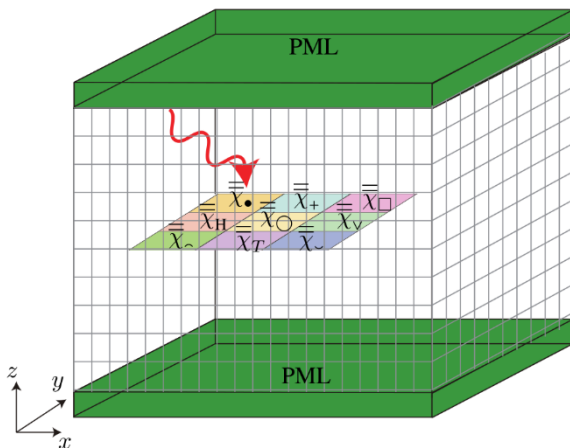
Our Solution



Modeling



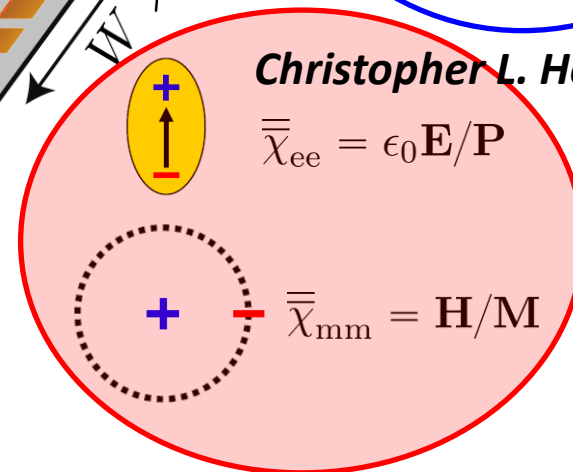
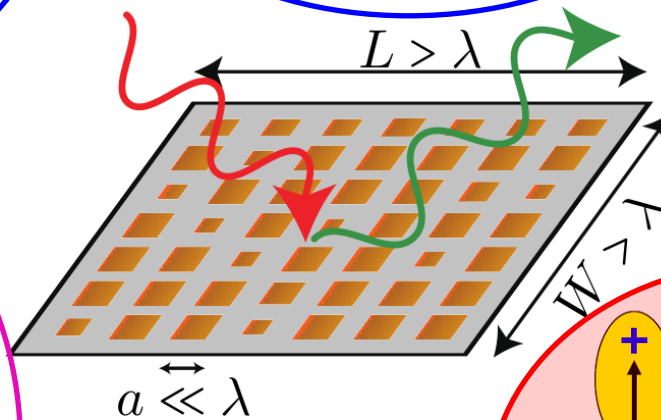
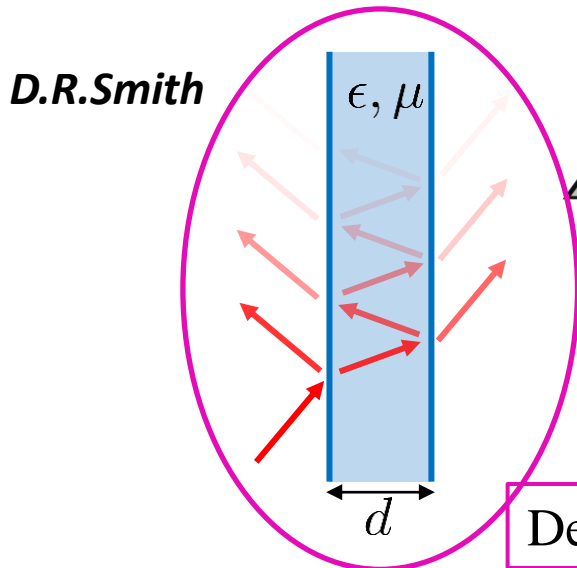
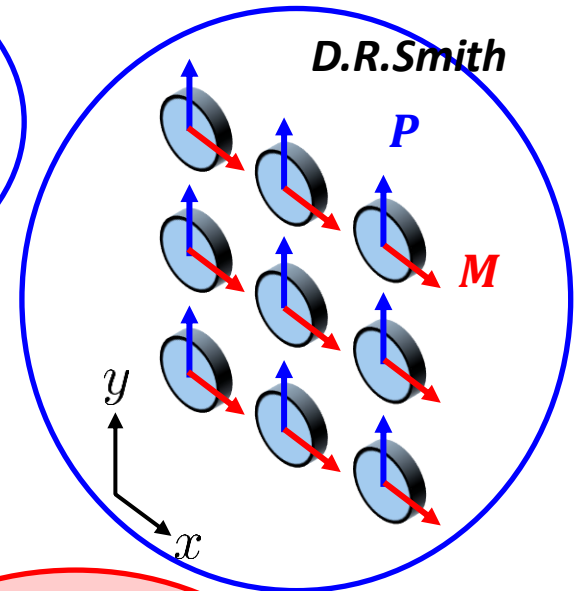
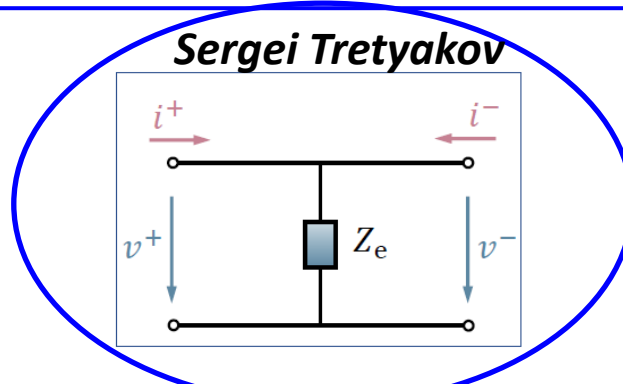
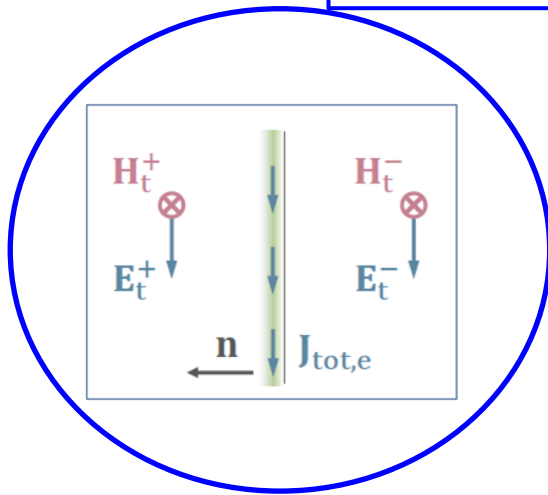
Inserting the model into numerical methods





Metasurfaces Modeling

Not intrinsic property, varying with incident waves

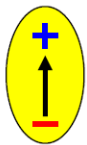
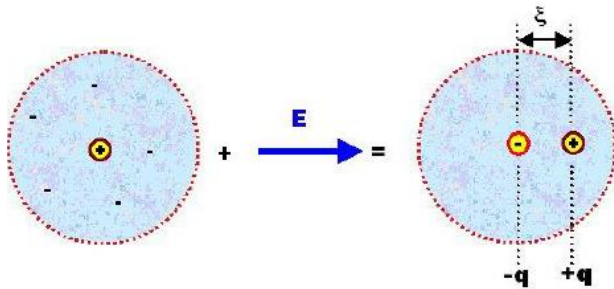


Dependent on d

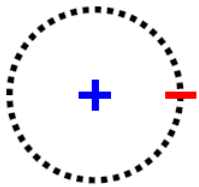


Surface Susceptibility Model

Material in nature

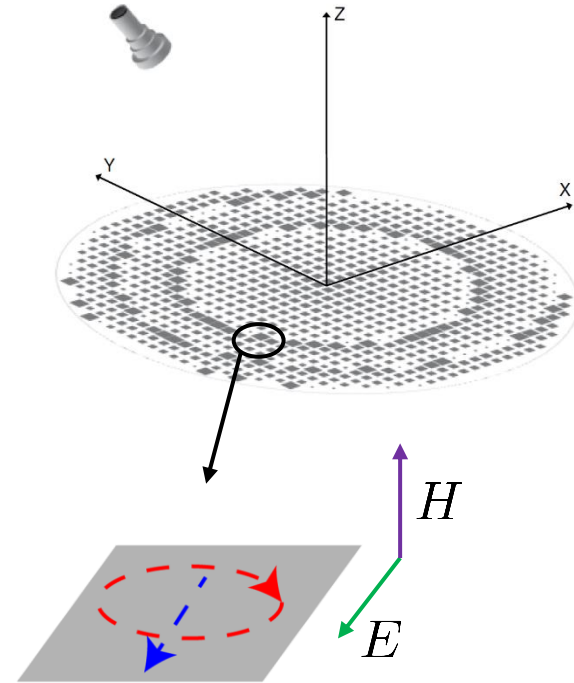


$$\mathbf{P} = \epsilon_0 \bar{\bar{\chi}}_{ee} \mathbf{E}$$



$$\mathbf{M} = \bar{\bar{\chi}}_{mm} \mathbf{H}$$

Artificial electromagnetic surface



$$\bar{\bar{\chi}}_{ee} = \epsilon_0 \mathbf{E}/\mathbf{P}$$

$$\bar{\bar{\chi}}_{mm} = \mathbf{H}/\mathbf{M}$$

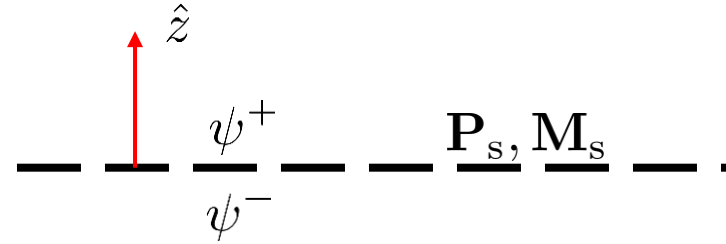
Ref: from slides for the lecture of electromagnetics and waves given by Prof. Fan Yang .



2D Form of Surface Susceptibility Tensor

$$\mathbf{P}_s = \epsilon_0 \bar{\bar{\chi}}_{ee} \mathbf{E}_{av} + \sqrt{\mu_0 \epsilon_0} \bar{\bar{\chi}}_{em} \mathbf{H}_{av}$$

$$\mathbf{M}_s = \sqrt{\epsilon_0 / \mu_0} \bar{\bar{\chi}}_{me} \mathbf{E}_{av} + \bar{\bar{\chi}}_{mm} \mathbf{H}_{av}$$



$$\Psi_{av} = \frac{\Psi^+ + \Psi^-}{2}, \quad \Psi = \mathbf{E}, \mathbf{H}$$

$$\bar{\bar{\chi}}_{ee} = \begin{bmatrix} \chi_{ee}^{xx} & \chi_{ee}^{xy} & \chi_{ee}^{xz} \\ \chi_{ee}^{yx} & \chi_{ee}^{yy} & \chi_{ee}^{yz} \\ \chi_{ee}^{zx} & \chi_{ee}^{zy} & \chi_{ee}^{zz} \end{bmatrix} \quad \bar{\bar{\chi}}_{mm} = \begin{bmatrix} \chi_{mm}^{xx} & \chi_{mm}^{xy} & \chi_{mm}^{xz} \\ \chi_{mm}^{yx} & \chi_{mm}^{yy} & \chi_{mm}^{yz} \\ \chi_{mm}^{zx} & \chi_{mm}^{zy} & \chi_{mm}^{zz} \end{bmatrix}$$

$$\bar{\bar{\chi}}_{em} = \begin{bmatrix} \chi_{em}^{xx} & \chi_{em}^{xy} & \chi_{em}^{xz} \\ \chi_{em}^{yx} & \chi_{em}^{yy} & \chi_{em}^{yz} \\ \chi_{em}^{zx} & \chi_{em}^{zy} & \chi_{em}^{zz} \end{bmatrix} \quad \bar{\bar{\chi}}_{me} = \begin{bmatrix} \chi_{me}^{xx} & \chi_{me}^{xy} & \chi_{me}^{xz} \\ \chi_{me}^{yx} & \chi_{me}^{yy} & \chi_{me}^{yz} \\ \chi_{me}^{zx} & \chi_{me}^{zy} & \chi_{me}^{zz} \end{bmatrix}$$



$$\bar{\bar{\chi}}_{ee} = \begin{bmatrix} \chi_{ee}^{xx} & \chi_{ee}^{xy} & 0 \\ \chi_{ee}^{yx} & \chi_{ee}^{yy} & 0 \\ 0 & 0 & 0 \end{bmatrix}$$

$$\bar{\bar{\chi}}_{mm} = \begin{bmatrix} 0 & 0 & 0 \\ 0 & 0 & 0 \\ 0 & 0 & \chi_{mm}^{zz} \end{bmatrix}$$

$$\bar{\bar{\chi}}_{em} = \begin{bmatrix} 0 & 0 & \chi_{em}^{xz} \\ 0 & 0 & \chi_{em}^{yz} \\ 0 & 0 & 0 \end{bmatrix}$$

$$\bar{\bar{\chi}}_{me} = \begin{bmatrix} 0 & 0 & 0 \\ 0 & 0 & 0 \\ \chi_{me}^{zx} & \chi_{me}^{zy} & 0 \end{bmatrix}$$

➤ Assumption 1: infinitely thin metafilm: $\rightarrow P_z = 0, M_x = 0, M_y = 0$

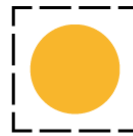
➤ Assumption 2: reciprocity $\rightarrow \bar{\bar{\chi}}_{ee}^T = \bar{\bar{\chi}}_{ee}, \bar{\bar{\chi}}_{mm}^T = \bar{\bar{\chi}}_{mm}, \bar{\bar{\chi}}_{me}^T = -\bar{\bar{\chi}}_{em}$



Bi-axial Susceptibility Tensor

$$\begin{aligned}\bar{\bar{\chi}}_{ee} &= \begin{bmatrix} \chi_{ee}^{xx} & \chi_{ee}^{xy} & 0 \\ \chi_{ee}^{yx} & \chi_{ee}^{yy} & 0 \\ 0 & 0 & 0 \end{bmatrix} \\ \bar{\bar{\chi}}_{mm} &= \begin{bmatrix} 0 & 0 & 0 \\ 0 & 0 & 0 \\ 0 & 0 & \chi_{mm}^{zz} \end{bmatrix} \\ \bar{\bar{\chi}}_{em} &= \begin{bmatrix} 0 & 0 & \chi_{em}^{xz} \\ 0 & 0 & \chi_{em}^{yz} \\ 0 & 0 & 0 \end{bmatrix} \\ \bar{\bar{\chi}}_{me} &= \begin{bmatrix} 0 & 0 & 0 \\ 0 & 0 & 0 \\ \chi_{me}^{zx} & \chi_{me}^{zy} & 0 \end{bmatrix}\end{aligned}$$

Bi-axial



$$\begin{aligned}\bar{\bar{\chi}}_{ee} &= \begin{bmatrix} \chi_{ee}^{xx} & 0 & 0 \\ 0 & \chi_{ee}^{yy} & 0 \\ 0 & 0 & 0 \end{bmatrix} \\ \bar{\bar{\chi}}_{mm} &= \begin{bmatrix} 0 & 0 & 0 \\ 0 & 0 & 0 \\ 0 & 0 & \chi_{mm}^{zz} \end{bmatrix} \\ \bar{\bar{\chi}}_{em} &= 0 \\ \bar{\bar{\chi}}_{me} &= 0\end{aligned}$$

Remarks:

1. The unknowns are reduced from 9 to 3 for bi-axial case.
2. Bi-axial case means that the structure do not generate cross polarization and transformation between electric to magnetic fields.

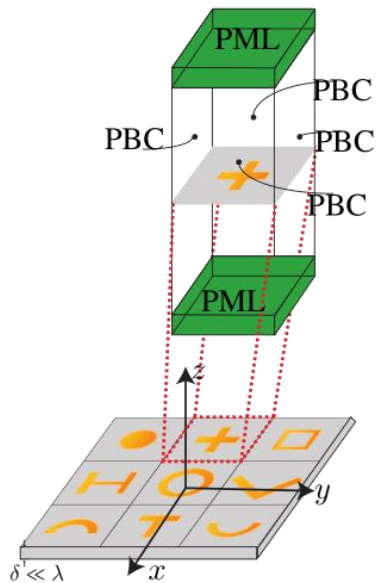


Surface susceptibility for bi-axial case

The relationship between surface susceptibility and reflection coefficients:

$$\text{TE}_z : R_{\text{TE}}^\theta = \frac{j\omega\epsilon_0\chi_{ee}^{yy}\eta + jk_0 \sin^2 \theta_i \chi_{mm}^{zz}}{-2 \cos \theta_i - j\omega\epsilon_0\chi_{ee}^{yy}\eta - jk_0 \sin^2 \theta_i \chi_{mm}^{zz}}$$

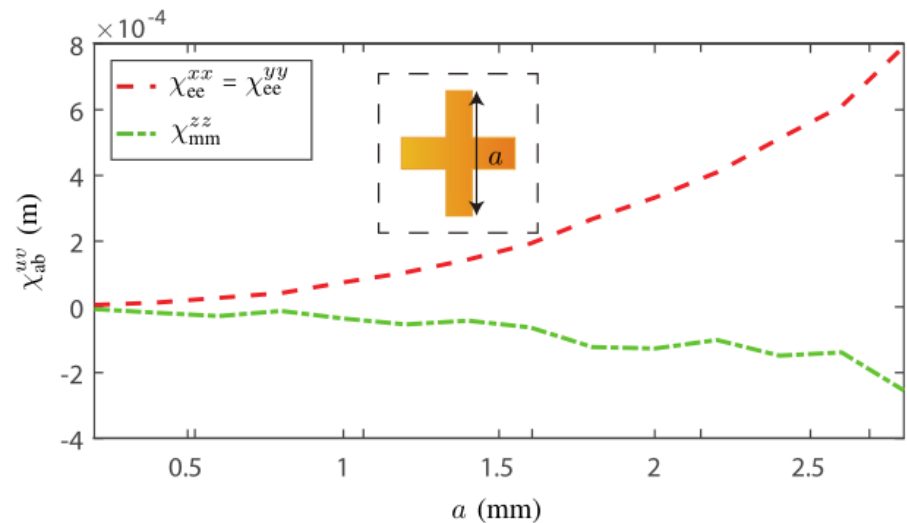
Two sets of simulation is required to extract the surface susceptibilities for bi-axial case:



$$\bar{\chi} = f(R)$$

$$\theta_i = 0 \rightarrow \chi_{ee}^{yy} = \chi_{ee}^{xx}$$

$$\theta_i = \theta_0 \rightarrow \chi_{mm}^{zz}$$



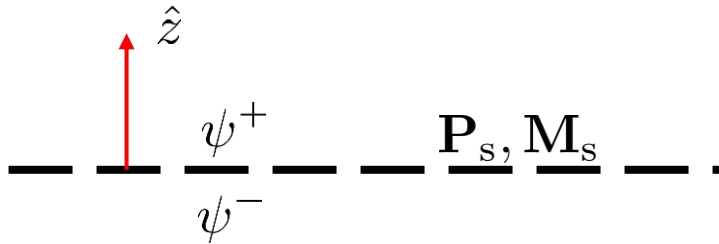


Outline

- ◆ Introduction of Metasurfaces
- ◆ Surface Susceptibility Model
- ◆ FDTD-SSM Algorithm
- ◆ Numerical Experiments
- ◆ Conclusion



SSM & Surface Currents



$$\Psi_{\text{av}} = \frac{\Psi^+ + \Psi^-}{2}, \quad \Psi = \mathbf{E}, \mathbf{H},$$

$$\mathbf{P}_s = \epsilon_0 \bar{\bar{\chi}}_{ee} \mathbf{E}_{\text{av}} + \sqrt{\mu_0 \epsilon_0} \bar{\bar{\chi}}_{em} \mathbf{H}_{\text{av}}$$

$$\mathbf{M}_s = \sqrt{\epsilon_0 / \mu_0} \bar{\bar{\chi}}_{me} \mathbf{E}_{\text{av}} + \bar{\bar{\chi}}_{mm} \mathbf{H}_{\text{av}}$$

Surface currents:

$$\mathbf{J}_{s,\text{tot}} = \mathbf{J}_{s,f} + \mathbf{J}_{s,p} + \mathbf{J}_{s,m}$$

$$= \mathbf{J}_{s,f} + \frac{\partial \mathbf{P}_{s,\parallel}}{\partial t} + (\nabla \times \mathbf{M}_s)_{\parallel} \quad (\text{A/m})$$

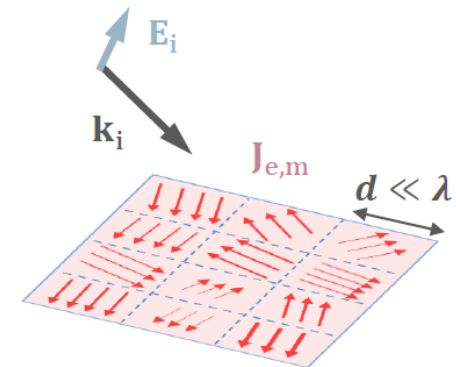
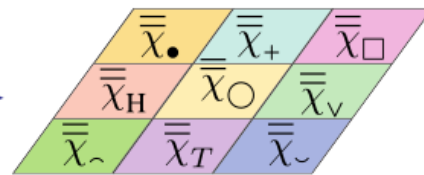
$$\mathbf{K}_{s,\text{tot}} = \mathbf{K}_{s,f} + \mathbf{K}_{s,m} + \mathbf{K}_{s,p}$$

$$= \mathbf{K}_{s,f} + \mu_0 \frac{\partial \mathbf{M}_{s,\parallel}}{\partial t} + [\nabla \times (\mathbf{P}_s / \epsilon_0)]_{\parallel} \quad (\text{V/m})$$

physical metasurface



$\bar{\bar{\chi}}$ -modeled metasurface



Ref 1: Idemen, M. Mithat. Discontinuities in the electromagnetic field. Vol. 40. John Wiley & Sons, 2011.

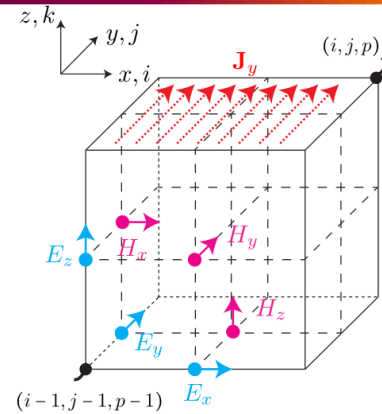
Ref 2: Achouri, Karim, Mohamed A. Salem, and Christophe Caloz. "General metasurface synthesis based on susceptibility tensors." IEEE Transactions on Antennas and Propagation 63.7 (2015): 2977-2991.

Ref 3: Kuester, Edward F., et al. "Averaged transition conditions for electromagnetic fields at a metafilm." IEEE Transactions on Antennas and Propagation 51.10 (2003): 2641-2651.



Surface currents in FDTD

$$\oint \mathbf{H} \cdot d\mathbf{l} = \epsilon_0 \iint \frac{\partial \mathbf{E}}{\partial t} \cdot d\mathbf{s} + \iint \mathbf{J}_s \cdot \delta(z) d\mathbf{s}$$



↓ Discretization in Yee cell

$$\begin{aligned} & (H_x^{n-1/2}(i, j, p) - H_x^{n-1/2}(i, j, p-1))\Delta x + (H_z^{n-1/2}(i, j, p) - H_z^{n-1/2}(i-1, j, p))\Delta z \\ &= \epsilon_0 \frac{E_y^n(i, j, p) - E_y^{n-1}(i, j, p)}{\Delta t} \Delta x \Delta z + J_y^{n-1/2}(i, j, p) \Delta x \end{aligned}$$

↓ Rearranging

$$\begin{aligned} E_y^n(i, j, p) &= E_y^{n-1}(i, j, p) + \frac{\Delta t}{\epsilon_0} \\ & \left[\frac{H_x^{n-1/2}(i, j, p) - H_x^{n-1/2}(i, j, p-1)}{\Delta z} - \frac{H_z^{n-1/2}(i, j, p) - H_z^{n-1/2}(i-1, j, p)}{\Delta x} \right] \\ & \quad + \frac{\Delta t}{\epsilon_0} \frac{J_y^{n-1/2}(i, j, p)}{\Delta z} \end{aligned}$$



Bi-axial SSM in FDTD

$$\mathbf{P} = \epsilon_0 \begin{bmatrix} \chi_{ee}^{xx} & 0 & 0 \\ 0 & \chi_{ee}^{yy} & 0 \\ 0 & 0 & 0 \end{bmatrix} \mathbf{E}, \quad \mathbf{M} = \begin{bmatrix} 0 & 0 & 0 \\ 0 & 0 & 0 \\ 0 & 0 & \chi_{mm}^{zz} \end{bmatrix} \mathbf{H}$$

$$\mathbf{J}_s = \frac{\partial \mathbf{P}}{\partial t} + \nabla \times \mathbf{M}$$

$$\rightarrow J_y = \left(\epsilon_0 \chi_{ee}^{yy} \frac{\partial E_y}{\partial t} - \frac{\partial(\chi_{mm}^{zz} H_z)}{\partial x} \right) \hat{y}$$

$$E_y^n(i, j, p) = E_y^{n-1}(i, j, p) + \frac{\Delta t}{\epsilon_0} \left[\frac{H_x^{n-1/2}(i, j, p) - H_x^{n-1/2}(i, j, p-1)}{\Delta z} - \frac{H_z^{n-1/2}(i, j, p) - H_z^{n-1/2}(i-1, j, p)}{\Delta x} \right]$$

$$- \frac{\Delta t}{\epsilon_0} \frac{J_y^{n-1/2}(i, j, p)}{\Delta z}$$

$$E_y^n(i, j, p) = E_y^{n-1}(i, j, p) + \frac{\Delta t \Delta z}{\epsilon_0 (\Delta z + \tilde{\chi}_{ee}^{yy}(i, j, p))} \left[\frac{H_x^{n-1/2}(i, j, p) - H_x^{n-1/2}(i, j, p-1)}{\Delta z} - \frac{H_z^{n-1/2}(i, j, p) - H_z^{n-1/2}(i-1, j, p)}{\Delta x} \right] +$$

$$\frac{\Delta t}{\epsilon_0 (\Delta z + \tilde{\chi}_{ee}^{yy}(i, j, p))} \frac{\chi_{mm}^{zz}(i, j, p) H_z^{n-1/2}(i, j, p) - \chi_{mm}^{zz}(i-1, j, p) H_z^{n-1/2}(i-1, j, p)}{\Delta x}$$

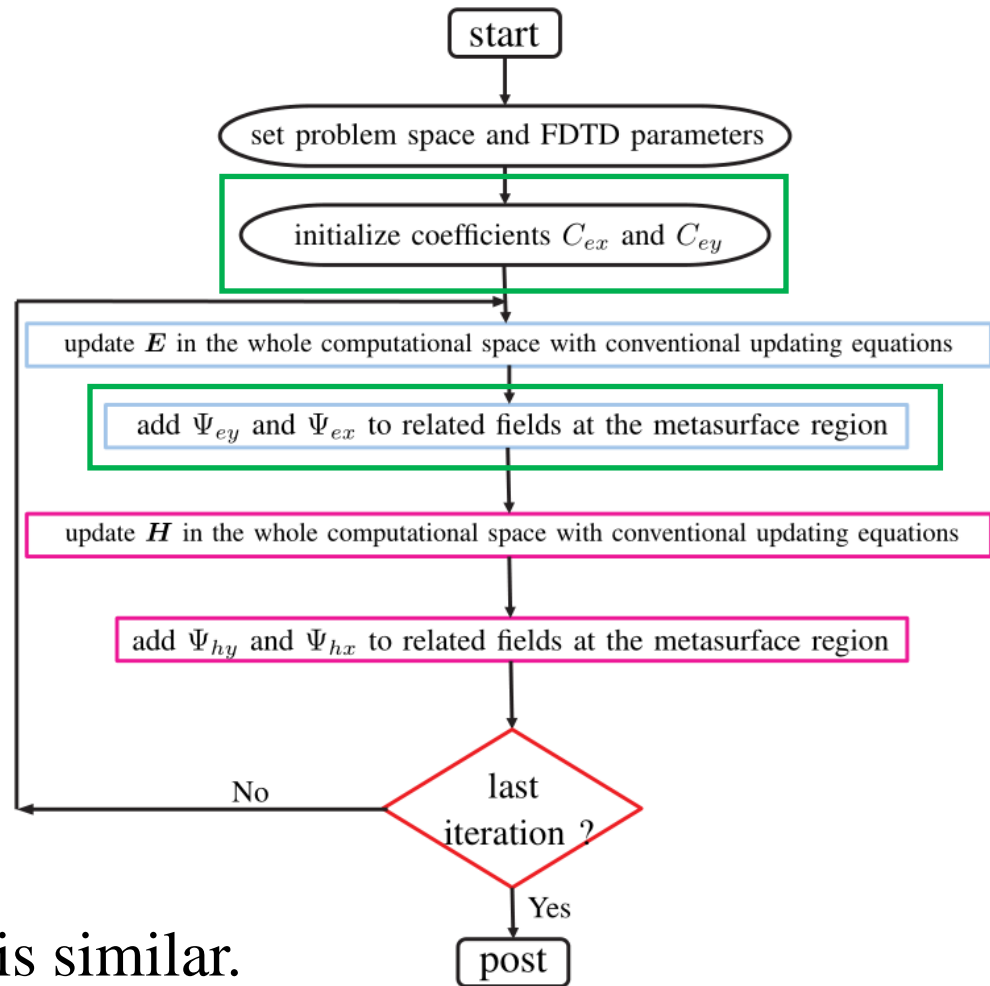


Flowchart of FDTD-SSM

$$C_{ey} = \frac{\Delta t \Delta z}{\epsilon_0 (\Delta z + \tilde{\chi}_{ee}^{yy}(i, j, p))}$$

$$\Psi_{ey} = \frac{\Delta t}{\epsilon_0 (\Delta z + \tilde{\chi}_{ee}^{yy}(i, j, p))} \frac{\chi_{mm}^{zz}(i, j, p) H_z^{n-1/2}(i, j, p) - \chi_{mm}^{zz}(i-1, j, p) H_z^{n-1/2}(i-1, j, p)}{\Delta x}$$

$$E_y^n(i, j, p) = E_y^{n-1}(i, j, p) + C_{ey} \left[\frac{H_x^{n-1/2}(i, j, p) - H_x^{n-1/2}(i, j, p-1)}{\Delta z} - \frac{H_z^{n-1/2}(i, j, p) - H_z^{n-1/2}(i-1, j, p)}{\Delta x} \right] + \Psi_{ey}$$



The updating procedure of E_x is similar.



Outline

◆ Introduction of Metasurfaces

◆ Surface Susceptibility Model

◆ FDTD-SSM Algorithm

◆ Numerical Experiments

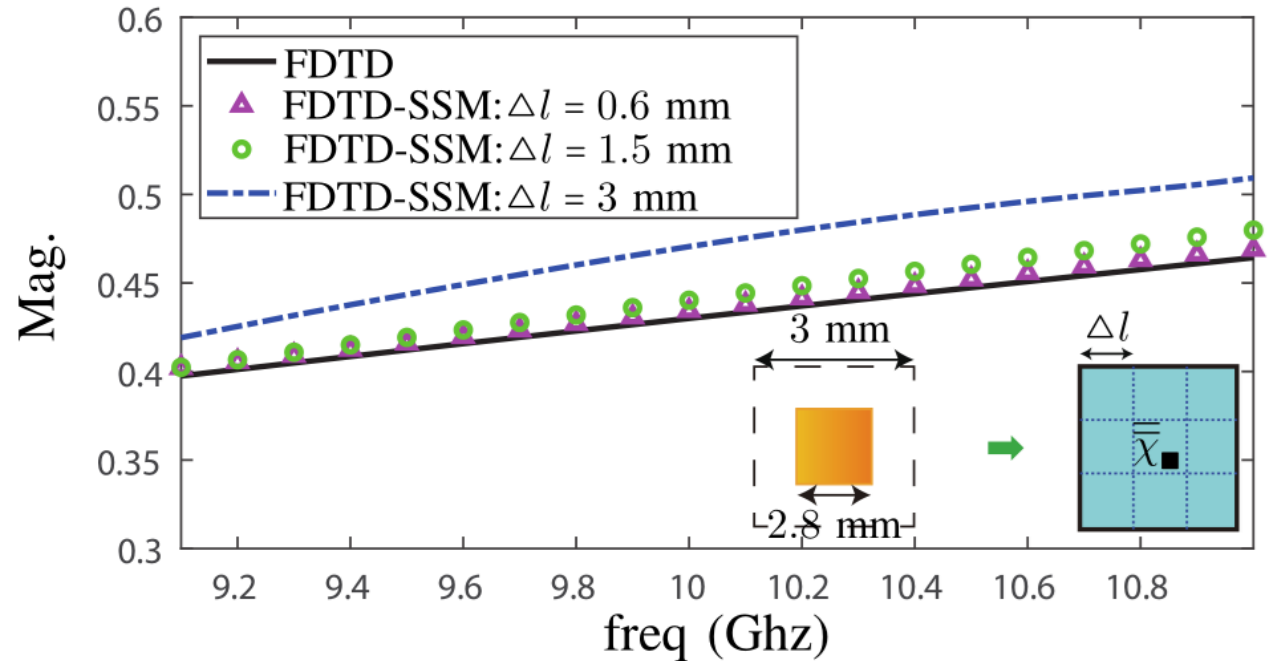
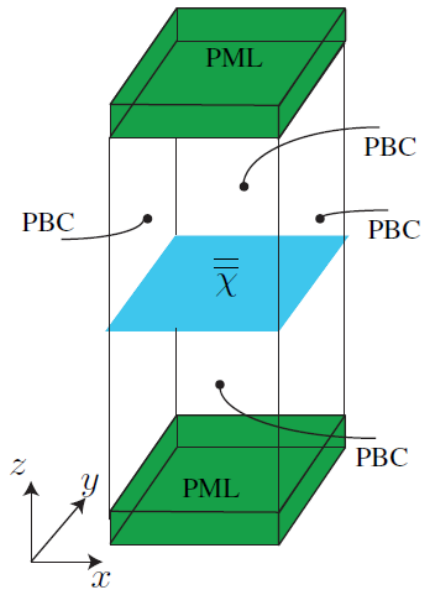
➤ Single layer

➤ Multi-layer

◆ Conclusion



Reduction of Meshing Lattice Size by using FDTD-SSM

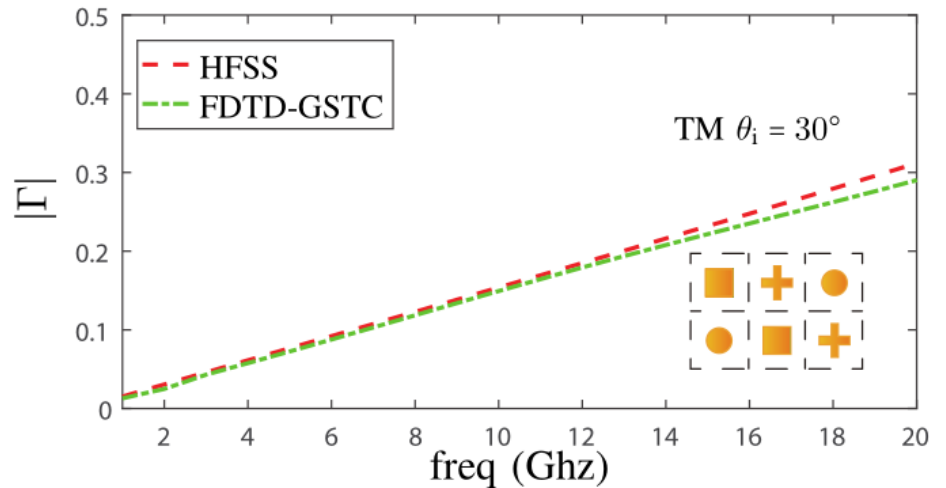
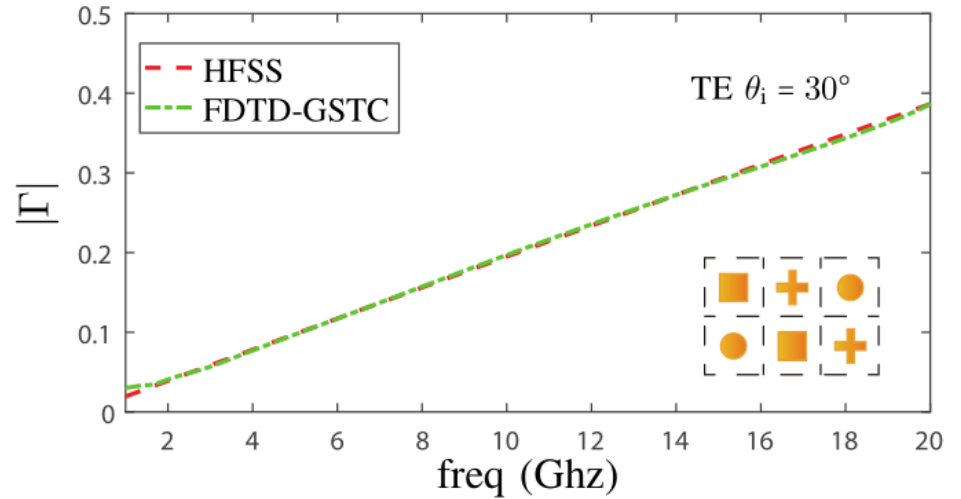
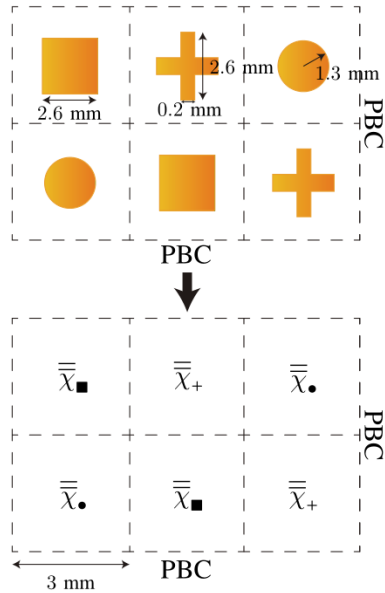


Remarks:

1. The meshing lattice size of conventional FDTD is $\frac{\lambda}{600} = 0.05\text{ mm}$.
2. As the meshing lattice size of FDTD-SSM decreasing to $\frac{\lambda}{50} = 0.6\text{ mm} = 12 \times 0.05\text{ mm}$, its results overlap with that of conventional FDTD.



The Accuracy of FDTD-SSM for Infinite Non-uniform Array

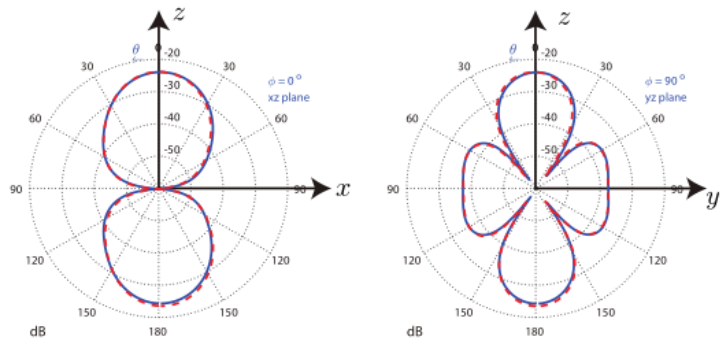
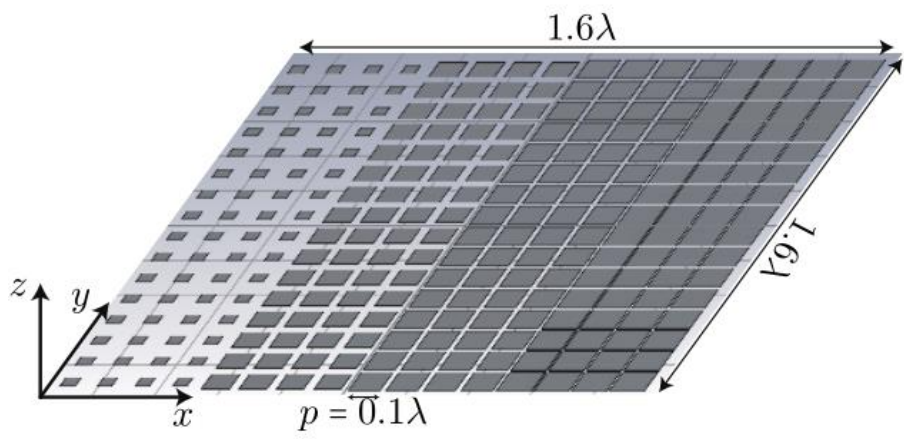


Remarks:

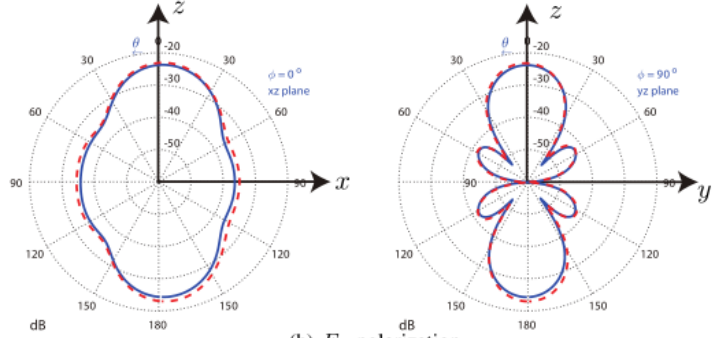
1. The FDTD-SSM is still valid even if the surrounding elements were changed.
2. The FDTD-SSM is valid for different incident angles and polarizations.



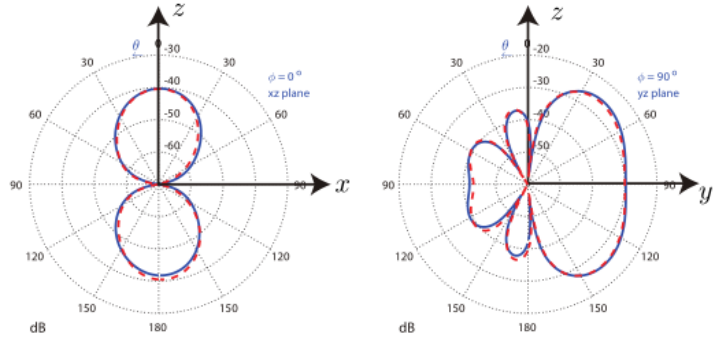
A Practical Application of FDTD-SSM for An Finite Array



(a) E_x polarization



(b) E_y polarization



(c) oblique incidence (E_x)



	cell size	time consum.
Conv. FDTD	$dx = dy = dz = 0.1 \text{ mm}$	(a) 2.5 hours (b) 2.5 hours (c) 6.3 hours
FDTD-SSM	$dx = dy = dz = 1.5 \text{ mm}$	(a) 35 seconds (b) 35 seconds (c) 53 seconds



Outline

◆ Introduction of Metasurfaces

◆ Surface Susceptibility Model

◆ FDTD-SSM Algorithm

◆ Numerical Experiments

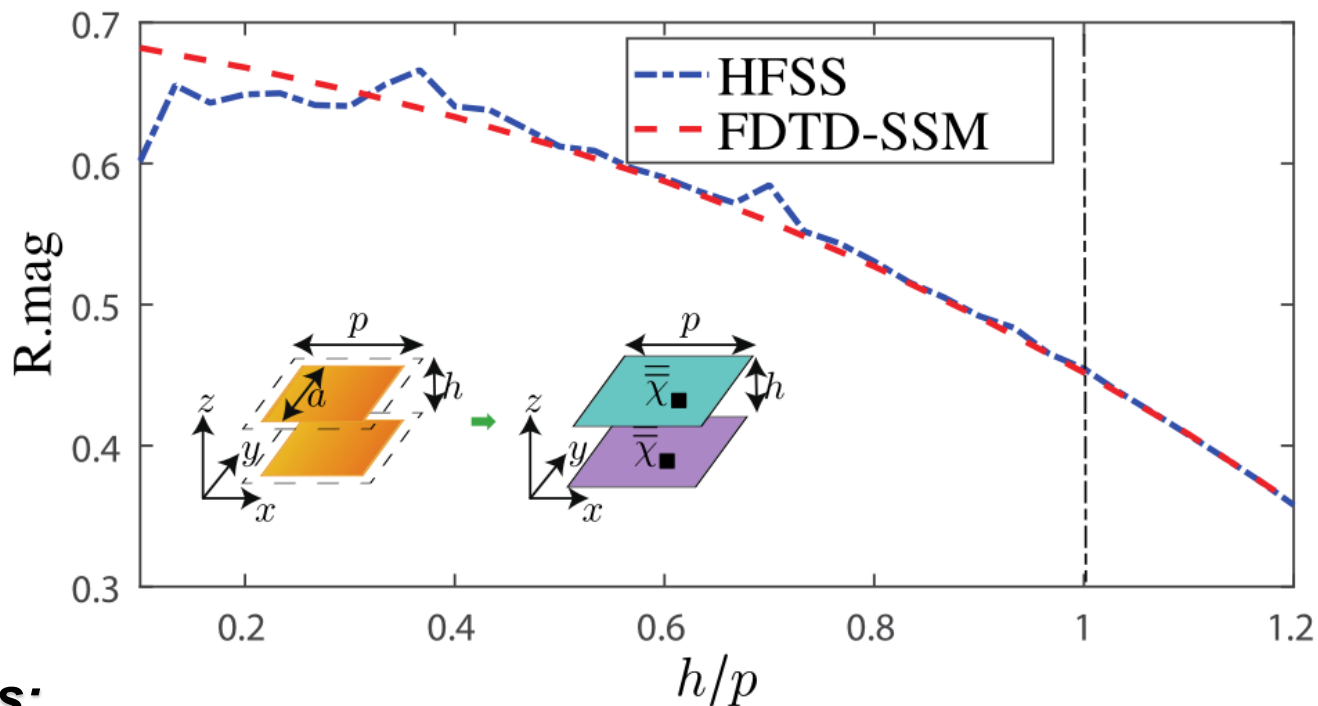
➤ Single layer

➤ Multi-layer

◆ Conclusion



Effective Distance Between Two Layers of SSM



Remarks:

1. A SSM simulation in **FDTD-SSM** is validated by a brute force simulation in **HFSS**.
2. If the distance between two layers is too small, the FDTD-SSM is not valid any more.
3. The FDTD-SSM is valid when the distance is bigger than one period.



Two-layer Structures Simulation

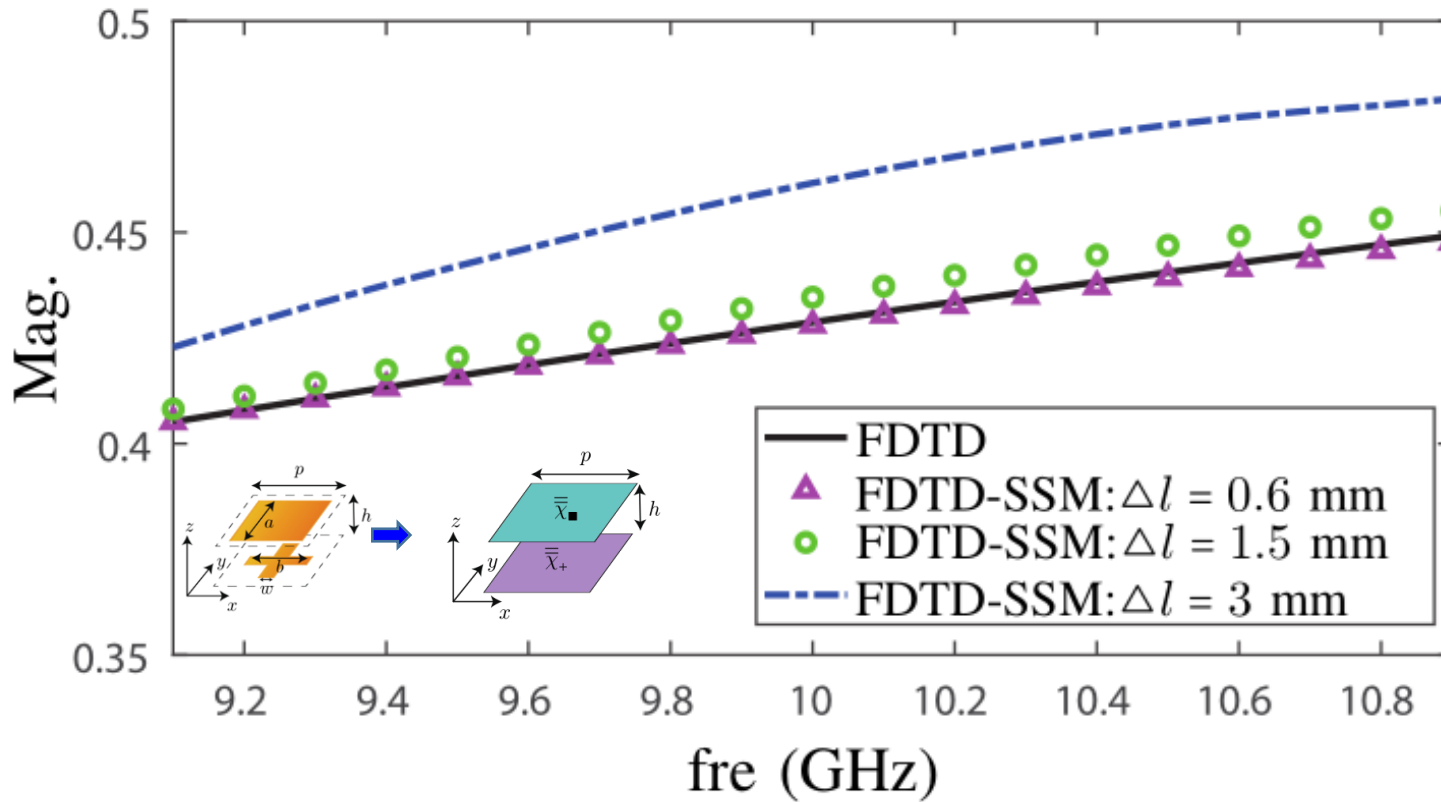


TABLE I
COMPUTATIONAL RESOURCES CONSUMPTION

	cell size	time consum.
Conv. FDTD	$dx = dy = dz = 0.05$ mm	2500 s
FDTD-SSM	$dx = dy = dz = 0.6$ mm	10 s



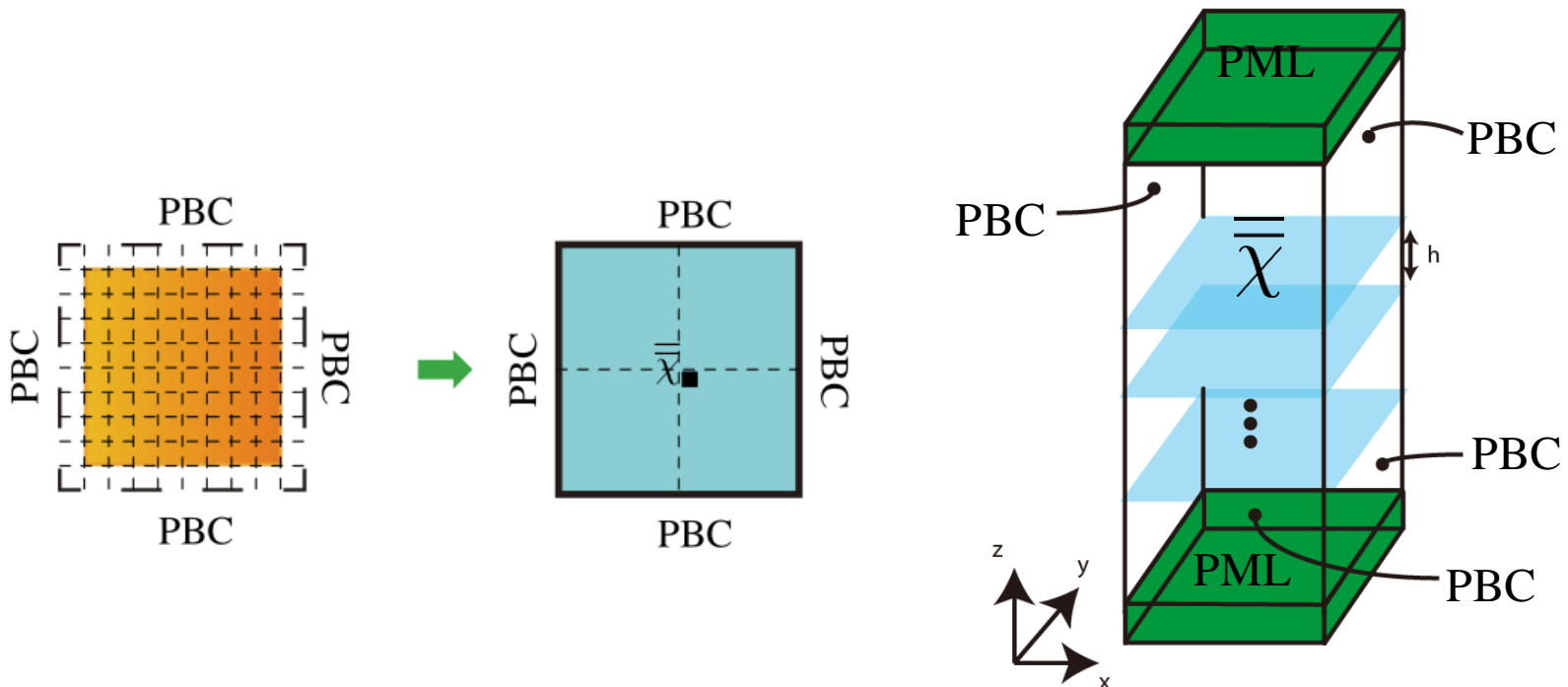
Outline

- ◆ Introduction of Metasurfaces
- ◆ Surface Susceptibility Model
- ◆ FDTD-SSM Algorithm
- ◆ Numerical Experiments
- ◆ Conclusion



Conclusion

- A novel FDTD-SSM algorithm for **accelerating** metasurface simulation.
 - Surface susceptibility model, extraction, surface currents in FDTD
 - Advantages: **simple & efficient**
- Applications of the FDTD-SSM algorithm
 - Reduction of meshing lattice size, effectiveness for different environment
 - Practical finite array, A six-layer structure
 - Consuming time is reduced **from hours to seconds**.





References

- [1] N. Yu and F. Capasso, “Flat optics with designer metasurfaces,” *Nat. Mater.*, vol. 13, no. 2, p. 139, 2014.
- [2] A. H. Abdelrahman, A. Z. Elsherbeni, and F. Yang, “Transmission phase limit of multilayer frequency-selective surfaces for transmitarray designs,” *IEEE Trans. Antennas Propag.*, vol. 62, no. 2, pp. 690–697, Feb 2014.
- [3] X. Jia, X. Liu, F. Yang, M. Li, and S. Xu, “FDTD simulation of metasurfaces with generalized sheet transition conditions,” in *Applied Computational Electromagnetics Society Symposium (ACES)*, 2017.
- [4] C. L. Holloway, E. F. Kuester, and A. Dienstfrey, “Characterizing metasurfaces/metafilms: The connection between surface susceptibilities and effective material properties,” *IEEE Antennas Wirel. Propag. Lett.*, vol. 10, pp. 1507–1511, 2011.
- [5] C. L. Holloway, E. F. Kuester, J. A. Gordon, J. O’Hara, J. Booth, and D. R. Smith, “An overview of the theory and applications of metasurfaces: The two-dimensional equivalents of metamaterials,” *IEEE Antennas Propag. Magazine*, vol. 54, no. 2, pp. 10–35, April 2012.
- [6] X. Liu, F. Yang, M. Li, and S. Xu, “Analysis of reflectarray antenna elements under arbitrary incident angles and polarizations using generalized boundary conditions,” *IEEE Antennas Wirel. Propag. Lett.*, vol. 17, no. 12, pp. 2208–2212, Dec 2018.



Thanks!